Vacuum annealing effect on physical properties and electrical circuit model of ZnO:Sn/SnO2:F bilayer structure

Samar Dabbabi, Mehdi Souli, Tarek Ben Nas, Antonio Garcia-Loureiro and Najoua Kamoun

Vacuum annealing effect on physical properties and electrical circuit model of ZnO:Sn/SnO_2:F bilayer structure

Samar Dabbabi[1], Mehdi Souli[1], Tarek Ben Nasr[1], Antonio Garcia-Loureiro[2], Najoua Kamoun[1]

1. Université Tunis El Manar, Faculté des Sciences de Tunis, Département de Physique, LR99ES13 Laboratoire de Physique de la Matière Condensée (LPMC), 2092 Tunis, Tunisia

2. Centro Singular de Investigación en Tecnoloxías de Información (CiTIUS), Universidad de Santiago de Compostela, España.

Corresponding author: samar.dabbabi@fst.utm.tn

Abstract:

Tin doped Zinc oxide/Fluorine doped tin dioxide bilayer films (ZnO:Sn/SnO_2:F) were deposited on glass substrates using spray pyrolysis technique. The effect of vacuum annealing at different temperature was investigated. Both structural and morphological analysis have shown that there is a significant modification in the bilayer film structure and surface following the vacuum annealing process at 450°C. Electrical properties have been investigated using the Hall Effect measurements as well as the impedance spectroscopy at room temperature. The circuit parameters were determined using an equivalent circuit model fitted from the impedance spectra and suggesting the presence of grain and grain boundary conductions in the bilayer structure. It was found that the film annealed in vacuum for 1h at 350°C is optimal in all respects, as it possesses all the desirable characteristics including the lowest resistivity, high porosity and better grain boundary conductivity.

Key words: Spray pyrolysis, ZnO:Sn/SnO_2:F film, Electrical properties, impedance spectroscopy.

Fabricating undoped or doped oxides in thin film form has long been a subject of many investigations for application in nanoelectronics [1], solar cells [2], acoustic devices

[3-4] and gas sensors [5-8]. Two metal oxides, namely zinc oxide (ZnO) and tin dioxide (SnO_2) are exceptional choices for fabrication of electronic devices [4, 9-10] with high performances, low cost and mass production [11-12]. The review of literature revealed that a double layered thin film composed of ZnO and SnO_2 doped with metals elements [11] and followed with annealing process [12] could give birth of the ideal electronic device where the crystallinity, the electrical conductivity and the morphological properties of ZnO/SnO_2 bilayers are improved compared to corresponding single layers and all other double layer films [1, 6]. Moreover, the ZnO/SnO_2 bilayer structure has been investigated for applications in the solar cells, photoelectrochemical cells (PECs), thin film transistors, gas sensors and nanogenerators [13-15]. P. Ravikumar et al. [15] fabricated SnO_2:Al/ZnO:F bi-layer with high transmittance, low resistivity, and homogeneity surface by employing spray pyrolysis technique and annealing process. The same result was obtained for ZnO:F/SnO_2:Al bi-layer [16]. In this work, the ZnO:Sn/SnO_2:F bi-layer films were fabricated by low cost spray pyrolysis and the effect of vacuum annealing temperature on structural, morphological and electrical were investigated. To the best of our knowledge, this is the first report following annealing process in vacuum on the ZnO:Sn/SnO_2:F double layered film. All bi-layered films were analyzed in terms of X-ray diffraction (XRD), Scanning electron microscopy study (SEM), and Hall Effect measurements. In order to investigate the device, the effects of vacuum annealing temperature on the complex impedance behavior were analyzed and an electrical model was proposed.

Spray pyrolysis technique was used to obtain the ZnO:Sn/SnO_2:F bilayer and its corresponding layers deposited on glass substrates. F-doped SnO_2 solution was prepared using 0.1 M of stannous chloride ($SnCl_2$:$2H_2O$) diluted in methanol (CH_3OH) and

deionized water (1:1). The fluorine doping was achieved using ammonium fluorine (NH_4F). On the other hand, Sn-doped ZnO solution was prepared using 0.1 M of zinc acetate dehydrate ($Zn(CH_3COO)_2.2H_2O$) diluted in methanol: deionized water (1:1) mixture. Stannous chloride ($SnCl_2:2H_2O$) was introduced as Sn dopant source. The addition of 6 at.% of F and 0.6 at.% of Sn have been optimized in SnO_2 and ZnO, respectively, achieving optimal material performance in terms of resistivity. Suitable volumes of ZnO:Sn precursor solution were sprayed over the SnO_2:F layers in order to get ZnO:Sn/SnO_2:F bilayer films. The samples were grown at the normalized deposition temperature of 450 °C. During the deposition run, the rate spray and the distance between the substrate and the nozzle were maintained constant at 20 ml min^{-1} and 25 cm, respectively. After the deposition, the samples have been annealed in vacuum better than 10^{-5} mbar at different temperatures. The structural characterization was performed by X-ray diffraction (XRD), using the copper radiation Kα (λ = 1.5418 A°) in the 2θ range 20–70° with a step size of 0.013° and a scan time per step of 2 s. The surface morphologies of the thin films were studied using Scanning Electron Microscopy (SEM, EVOLSIS Zeiss). SEM cross section was performed to measure the film thickness. Electrical parameters of the films were measured by four probe, in a Van der Pauw configuration. The impedance measurements were performed using two-electrodes painted on the two extremities of the film using silver paste. The impedance data was determined using Agilent E4980A impedance analyzer at room temperature in the frequency range [20 Hz - 2 MHz].

The X-ray patterns and the structure of the fabricated ZnO:Sn/SnO_2:F bi-layer films are shown in Fig.1a and the inlet, respectively. Fig.1b shows XRD patterns of bilayer film annealed at different temperatures under vacuum for 1h. Fig.1a suggests that

ZnO:Sn/SnO_2:F film is polycrystalline. All diffraction peaks can be perfectly indexed as the hexagonal wurzite phase of ZnO:Sn (JCPDS 89-1397) as well as the tetragonal rutile structure of SnO_2:F phase (JCPDS 41-1445). Major diffraction peaks at angles 2θ around 26.32°, 33.62°, 37.72°, 51.44°, 64.57° and 65.62° belong to the planes {110}, {101},{200}, {211}, {310} and {301} of SnO_2:F. The small reflection peaks at angles around 31.58°, 34.23°, 36.03°, 47.33°, 56.47° and 62.62° correspond to {100}, {002}, {101}, {102},{110} and {103} planes of ZnO:Sn, respectively. The same result was obtained by Hossein et al. [17]. As shown in Fig.1b, the crystal structure of ZnO:Sn/SnO_2:F film annealed at 250 °C was identified to that of as-grown film, whereas with the increase in the annealing temperature at 350°C, the position of all diffractions peaks were observed to decrease drastically. The shift in the diffraction peaks position is due to the stress changing in the film [18]. By increasing annealing temperature at 450°C, we observed the formation of amorphous phase in the bi-layer film. Thus, the vacuum annealing process at 450°C inhibits the crystallite growth of ZnO:Sn on SnO_2:F. Cross-sectional SEM image of the prepared ZnO:Sn/SnO_2:F bi-layer film is shown in Fig. 2. As indicated in this image, the thickness value is 918.2 nm for all the deposited bi-layer films. The influence of vacuum annealing for a period of 1h on the surface morphology is shown in Fig.3. The as-deposited film (Fig.3a) exhibited a tiny chilly like structures with homogeneous surface. It is clear that the surface of the film annealed at 350°C (Fig.3c) is much smoother and more uniform than as-deposited thin film. However, these tiny chilly like structures become bigger and they are protuberant at 450°C temperature (Fig.3d). When the films are annealed in vacuum at high temperature, grains get agglomerated to form small clusters then it results in an increase in the grain size [19, 20] which could explain the case of the film annealed at 450°C under vacuum atmosphere. These results

corroborated well with our XRD findings, by which an amorphous structure was observed at 450°C annealing temperature.

The electrical parameters like the resistivity (ρ), carrier concentration (N), mobility (μ) and electrical conductivity (σ) were obtained using Hall Effect measurements. Fig.4 presents the variation of electrical parameters of the prepared films as function of annealing temperatures used in vacuum for 1h. Firstly, the resistivity decreased with increasing annealing temperature and then it increased at high temperature of 450°C. A minimum resistivity of 0.05×10^{-2} Ω.cm is obtained for ZnO:Sn/SnO_2:F bilayer annealed at 350 °C. The conductivity exhibited the opposite behavior as revealed in Fig.4. It is seen that the carrier concentration exhibited 4×10^{24} cm^{-3} value saturated at 350 °C and 450 °C temperatures, which is lower than that at 250 °C ($7\times10^{24}cm^{-3}$). While, the highest Hall mobility ($\mu = 0.7\times10^{-8}$ $cm^2V^{-1}s^{-1}$) is obtained for the film annealed at 350 °C. The film annealed at 450 °C exhibits a low mobility as compared to that at 350 °C, possibly due to their being more disordered in terms of crystallinity [20]. It is obvious from these results that the vacuum annealing at 350 °C temperature promote higher mobility and less resistivity for the ZnO:Sn/SnO_2:F bilayer.

Electrochemical impedance spectroscopy (EIS) is a powerful tool for studying the device interface information [21]. Fig.5 (a-d) show the impedance spectra or the Nyquist diagram of ZnO:Sn/SnO_2:F based devices with and without vacuum annealing temperature. It is observed that the impedance spectra of all these films are characterized by a single semicircular arc. The center of each observed semi-circle is shifted down to the real axis confirming that the impedance curves of this bi-layer film obey the Cole-Cole formalism [22]. The presence of only one semicircle in the Cole-Cole plot represents the Debye relaxation process [23]. In order to identify the contribution of each compound of the

material (grain, grain boundary, and electrodes), it is useful to have an equivalent circuit model [24]. In this regards, the impedance curves were fitted by using Zview software [24], to an equivalent circuit consisting of a series resistance (R1) and a capacitance (CPE1) in parallel with a resistance (R2) as indicated in the insets of Fig.5 (a-d). The grains contribute at high frequencies, the grain boundaries at intermediate frequencies and electrodes at low frequencies [25]. The electrical parameters R1, CPE1, and R2 represent the contribution of the electrodes, grain and grain boundary, respectively. The values of these parameters are illustrated in Fig.5 (a-d). It is observed that as annealing temperature increases in the range of [250-350°C], the grain resistances decrease. The lowest R2 value is 0.078 $\times 10^3$ Ω which was obtained for the film annealed at 350°C. However, the increase annealing temperature at 450°C induce the reduction of R2 value or the grain resistance. This enhancement in conductivity at 350°C temperature is also confirmed from the Hall effect analyzes. To the best of our knowledge, it was not found in the bibliography a similar study to compare our obtained values which mark the originality of our work.

In this study, we have studied the effect of annealing under vacuum atmosphere at 250, 350 and 450 °C on structural, morphological and electrical behavior of ZnO:Sn/SnO_2:F bilayer thin films. The X-ray diffraction analysis revealed that the vacuum annealing process at 250°C and 350°C resulting in polycrystalline materials, while the film annealed at 450°C leads to an amorphous phase. This significant modification was strongly supported by the surface morphological results. Electrical properties of this bilayer were performed using Hall Effect measurements as well as complex impedance spectroscopy. As a result, a minimum resistivity of 0.05×10^{-2} Ω.cm

and an enhanced grain boundary conductivity were achieved for the film annealed at 350°C under vacuum gas condition.

Acknowledgements

The Authors would like to thank the use of RIAIDT-USC analytical facilities at the University of Santiago de Compostela. Authors are also grateful to (Francisco Rivadulla and Victor Leborán, CIQUS-USC) for assisting us with the Hall Effect measurements.

References

[1] G. Giusti, V. Consonni, ACS Appl. Mater. Interfaces. 6 (2014) 14096–14107. doi:10.1021/am5034473.

[2] N. Chantarat,a Shu-Han Hsu, J.M. Chem, (2012) 8005–8012. doi:10.1039/c2jm15682b.

[3] A. Kudret, S. Tekerek, J. Phys. Chem. Solids. 72 (2011) 701–704. doi:10.1016/j.jpcs.2011.02.017.

[4] T. Tharsika, A.S.M.A. Haseeb, M.F.M. Sabri, Thin Solid Films. 558 (2014) 283–288. doi:10.1016/j.snb.2016.08.158.

[5] L.F. da Silva, S. Bernardini, V.R. Mastelaro, K. Aguir, C. Ribeiro, E. Longo, B Chem. 240 (2017) 573–579. doi:10.1016/j.tsf.2014.02.022.

[6] Luís F. da Silva, Mattia A. Lucchini, Jean-Claude M'Peko, Sandrine Bernardini, Khalifa Aguir, Caue Ribeiro, Elson Longo and Markus Niederberger, Proceedings. 1 (2017) 418. doi:10.3390/proceedings1040418.

[7] P. Zhang, G. Pan, B. Zhang, J. Zhen, Y. Sun, Materials Research. 17 (2014) 817-822. doi: 10.1590/1516-1439.235713.

[8] M.K. Verma, V. Gupta, Proc. IMCS 2012. (2012) 787–790. doi: 10.5162/IMCS2012/P1.0.13.

[9] A. Paliwal, A. Sharma, M. Tomar, V. Gupta, Sensors Actuators, B Chem. 250 (2017) 679–685. doi:10.1016/j.snb.2017.05.064.

[10] S.M.H. Al-Jawad, Optik (Stuttg). 146 (2017) 17–26.

doi:10.1016/j.ijleo.2017.08.053.

[11] E. Espid, F. Taghipour, ECS J. Solid State Sci. Technol. 7 (2018) Q3089–Q3093. doi:10.1149/2.0141807jss.

[12] E. Peksu, H. Karaagac, J. Alloys Compd. 764 (2018) 616–625. doi:10.1016/j.jallcom.2018.06.101.

[13] J. Kaur, R. Kumar, M.C. Bhatnagar, Sensors Actuators, B Chem. 126 (2007) 478–484. doi:10.1016/j.snb.2007.03.033.

[14] S.K. Sinha, T. Rakshit, S.K. Ray, I. Manna, Appl. Surf. Sci. 257 (2011) 10551–10556. doi:10.1016/j.apsusc.2011.07.049.

[15] P. Ravikumar, K. Ravichandran, B. Sakthivel, N.J. Begum, A.T. Ravichandran, J. Mater. Sci. Mater. Electron. 24 (2013) 4092–4097. doi:10.1007/s10854-013-1366-0.

[16] P. Ravikumar, K. Ravichandran, B. Sakthivel, J. Mater. Sci. Technol. 28 (2012) 999–1003. doi: https://doi.org/10.1016/S1005-0302(12)60164-9.

[17] H. Mahmoudi Chenari, R. Zamiri, D. Maria Tobaldi, M. Shabani, A. Rebelo, J.S. Kumar, S.A. Salehizadeh, M.P.F. Graça, M.J. Soares, J. António Labrincha, J. Sol-Gel Sci. Technol. 84 (2017) 274–282. doi:10.1007/s10971-017-4484-y.

[18] A.B. Yadav, K. Singh, A. Pandey, S. Jit, Superlattices Microstruct. 71 (2014) 250–260. doi:10.1016/j.spmi.2014.03.043.

[19] H.W. Lee, W.J. Cho, AIP Advances 8 (2018) 015007. doi:10.1063/1.5009895.

[20] K. Ravichandran, R. Mohan, N.J. Begum, S. Snega, K. Swaminathan, C. Ravidhas,

B. Sakthivel, S. Varadharajaperumal, Vacuum 107 (2014) 68-76 doi:10.1016/j.vacuum.2014.03.029.

[21] A.Tataroğlu, Microelectronic Engineering. 83 (2006) 2551-2557. doi: https://doi.org/10.1016/j.mee.2006.06.007.

[22] Jendoubi, I., Ben Smail, R., Maczka, M. et al. Ionics. 24(2018) 24-3515. doi: 10.1142/S2010135X12300149.

[23] S. Pati, International Journal on Recent and Innovation Trends in Computing and Communication ISSN. 3 (2015) 2321-8169. http://www.ijritcc.org/.

[24] L. Troncoso, J. A. Alonso and A. Aguaderob, J. Mater. Chem. A. 3 (2015) 17797-17803. doi: 10.1039/C5TA03185K.

[25] K. Sahoo, J. Majhi, A. Mitra, A.S. Kumar, Journal of The Electrochemical Society. 166 (2019) A342-A352. doi: 10.1149/2.1161902jes.

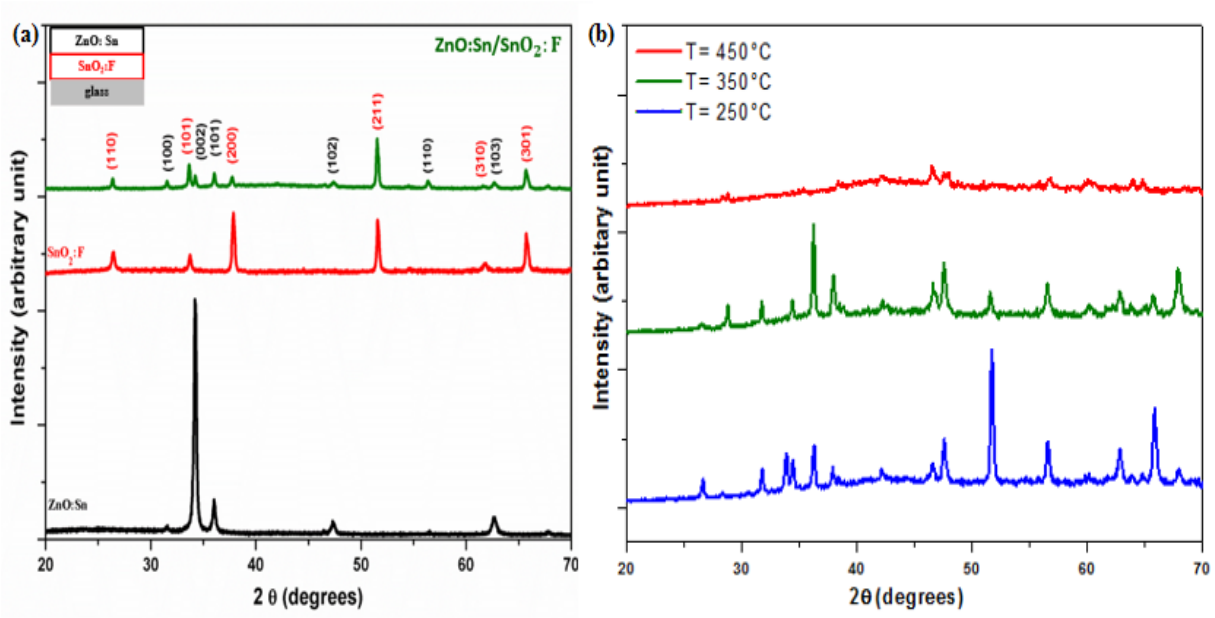

Fig.1. X-ray diffraction spectra of (a) ZnO:Sn/SnO_2:F bilayer and its corresponding single layers, (b) ZnO:Sn/SnO_2:F annealed for 1h in vacuum at different temperatures.

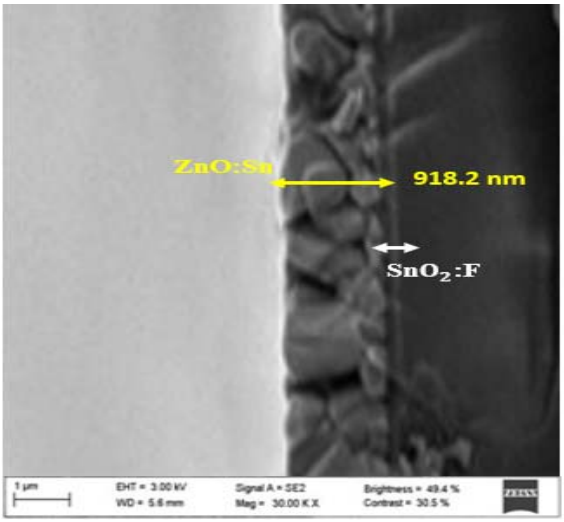

Fig.2. SEM cross section image of ZnO:Sn/SnO_2:F bilayer.

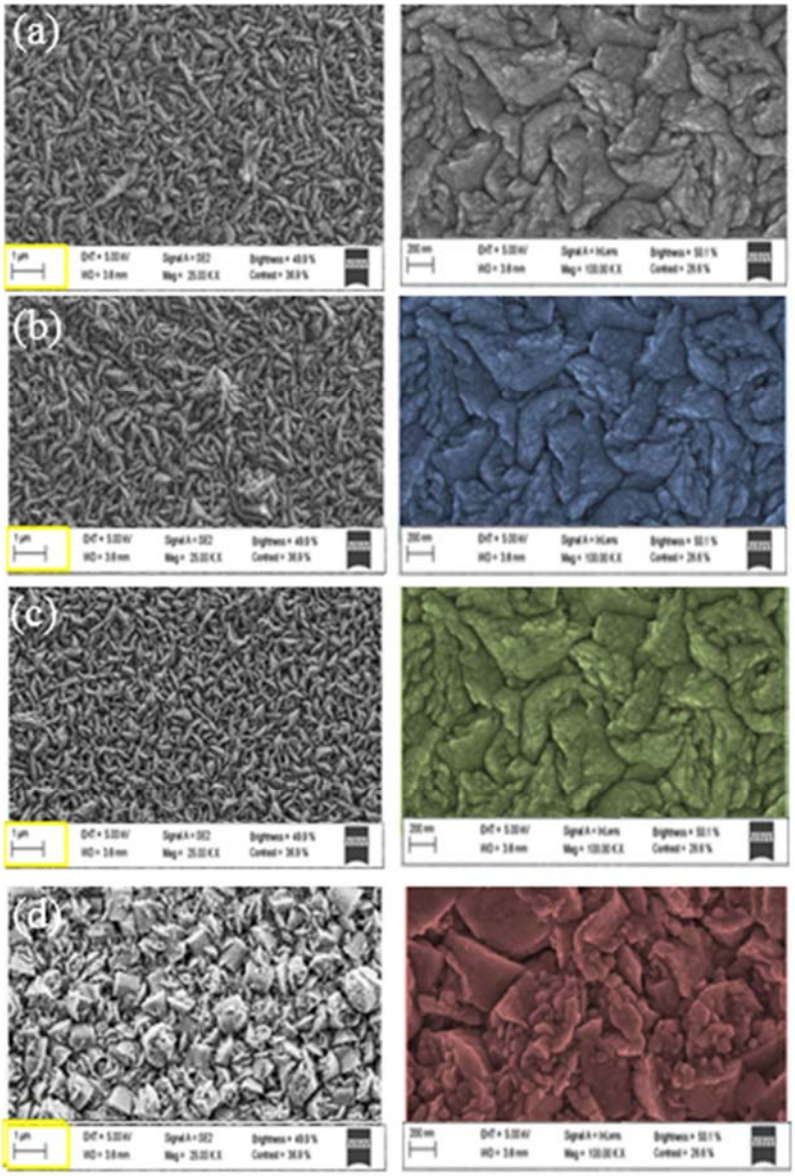

Fig.3. Plan-view SEM images of the ZnO:Sn/SnO_2:F bilayer (a) as grown and annealed for 1h in vacuum at (b) 250°C, (c) 350°C and (d) 450°C.

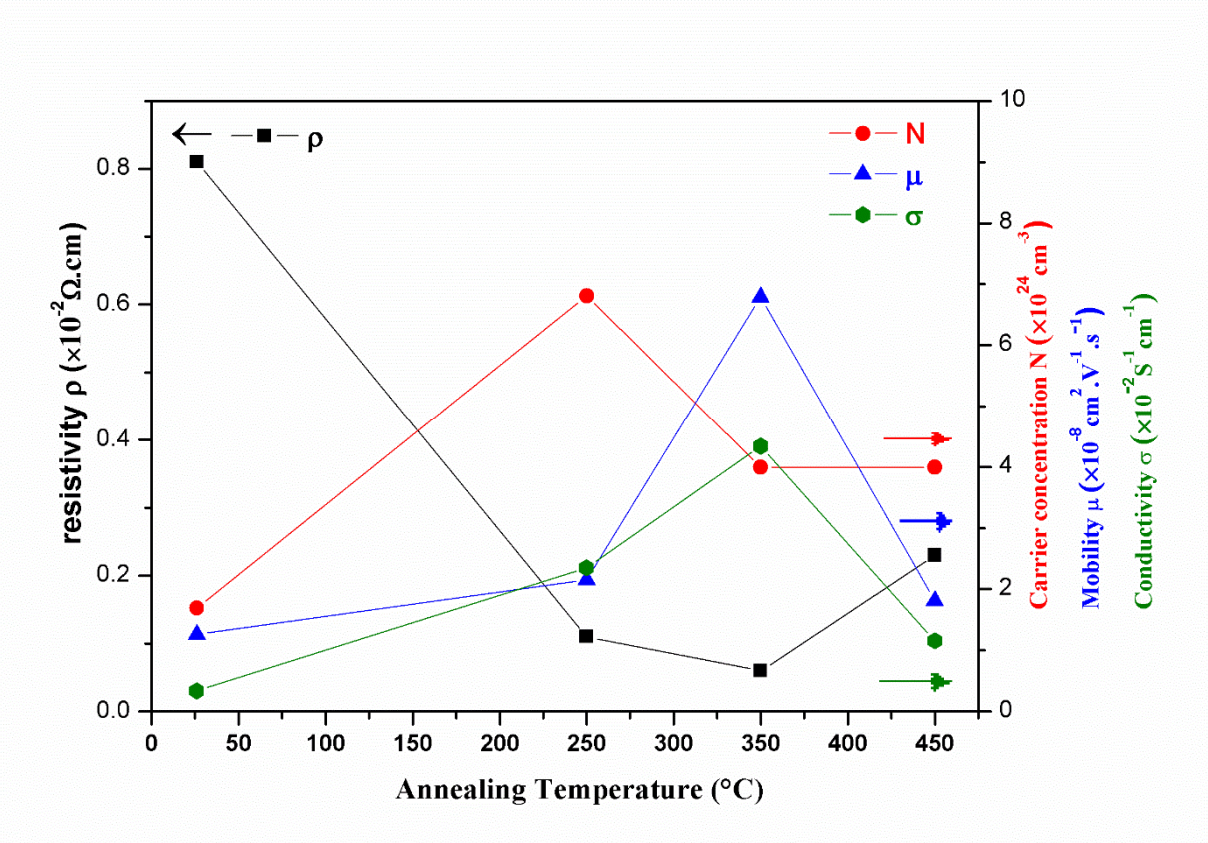

Fig.4. Resistivity, carrier concentration, mobility and conductivity as a function of vacuum annealing temperatures for ZnO:Sn/SnO_2:F bilayer.

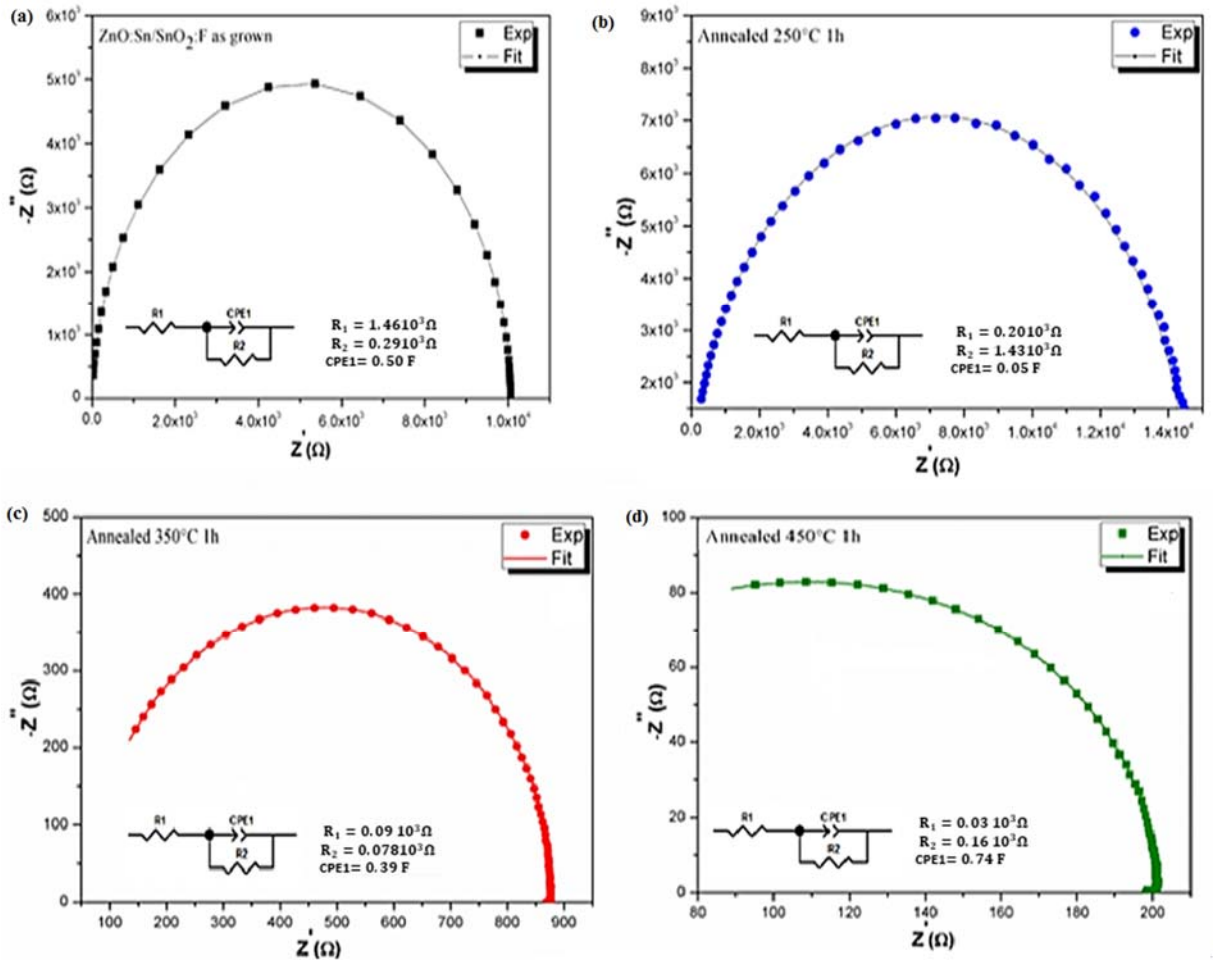

Fig.5. Complex impedance spectra of ZnO:Sn/SnO_2:F bilayer (a) as grown and annealed for 1h in vacuum at (b) 250°C, (c) 350°C and (d) 450°C.